AIR DAMPING EFFECTS ON DIFFERENT MODES OF AlN-on-Si MICROELECTROMECHANICAL RESONATORS

Yuncong Liu[1†], S M Enamul Hoque Yousuf[1†*], Afzaal Qamar[2], Mina Rais-Zadeh[2,3*], and Philip X.-L. Feng[1*]*

[1]Electrical & Computer Engineering, University of Florida, Gainesville, FL 32611, USA
[2]Electrical & Computer Engineering, University of Michigan, Ann Arbor, MI 48109, USA
[3]Jet Propulsion Laboratory, California Institute of Technology, Pasadena, CA 91109, USA

2023 IEEE 36th International Conference on Micro Electro Mechanical Systems (MEMS) | 978-1-6654-9308-6/23/$31.00 ©2023 IEEE | DOI: 10.1109/MEMS49605.2023.10052273

ABSTRACT

Piezoelectric thin films have enabled demonstrations of a wide range of piezoelectric-on-silicon (PoS) resonant transducers in microelectromechanical systems (MEMS) industry today. While the actual ambient pressure (p) levels in vacuum packages can greatly affect device performance, a comprehensive study and quantitative understanding of dynamical characteristics of multimode PoS resonators under varying pressure is still lacking and needs to be investigated. In this work, we report the first measurements and analyses of air damping effects on both bulk and flexural resonance modes of AlN-on-Si (AlN/Si) bulk acoustic resonators (BARs). Experimental results are presented for the resonant frequency (f) and quality (Q) factor with p varying from 760Torr down to 100μTorr. For AlN/Si resonator's bulk mode, f keeps a nearly constant value of 10.291MHz over the pressure range and the Q factor starts to decline when p is above 10Torr. For AlN/Si resonator's flexural mode, f is stable at 595.3kHz below 20Torr and drops to 595kHz at 760Torr. For the Si-only device's bulk mode, f ~10.127MHz is independent of p, and a high Q ~257,000 is maintained when p < 3Torr. The present work clearly reveals the different effects that air damping exerts upon the bulk and flexural modes of AlN/Si MEMS resonators, providing new quantitative knowledge and insight for device engineering.

KEYWORDS

Micromechanical resonator, air damping, aluminum nitride (AlN), piezoelectric resonator, quality (Q) factor.

INTRODUCTION

Thin film piezoelectric resonators have attracted a considerable amount of interest and are relevant to a broad variety of applications in communication, timing, sensing, and energy harvesting [1-3]. Among the important thin film materials with strong piezoelectricity, AlN is appealing for various radio-frequency (RF) applications also thanks to its high thermal conductivity, strong electric insulation properties, and ease of fabrication at scale [3]. Combining excellent electromechanical coupling of AlN with low acoustic loss of single crystal Si, AlN/Si BARs can exhibit high power handling and compatibility with mainstream CMOS wafer-scale manufacturing [4]. To maximize the benefits of the exceptional properties of laterally vibrating AlN/Si resonators, high-Q modes are preferable for more precise sensing and better frequency selection. Pursuing such high-Q devices requires carefully investigating and understanding the limits of loss mechanisms. Various energy loss mechanisms can contribute to the overall dissipation in such devices, which can be expressed as:

$$\left(\frac{1}{Q}\right)_{\text{tot}} = \left(\frac{1}{Q}\right)_{\text{med}} + \left(\frac{1}{Q}\right)_{\text{ted}} + \left(\frac{1}{Q}\right)_{\text{al}} + \left(\frac{1}{Q}\right)_{\text{others}}, \quad (1)$$

where it identifies three main dissipation mechanisms: medium (*i.e.*, air) damping Q^{-1}_{med}, thermoelastic damping Q^{-1}_{ted}, and anchor loss Q^{-1}_{al}. It has been shown that the thermoelastic damping from columnar boundaries in the AlN piezoelectric layer causes Q of AlN/Si device to be lower than that of Si-only device [5]. Further, inclusion of metal electrodes atop the AlN/Si heterostructure, as is typically needed for piezoelectric excitation and detection of resonant motions, can significantly lower the Q [6]. To address this issue and retain high Q, we have demonstrated a non-contact electrical excitation scheme recently [6], where an external electrode is devised to efficiently drive the length extensional (LE) and other vibrational modes of the electrode-less resonator, via inverse piezoelectric effect and gradient force from the electric field.

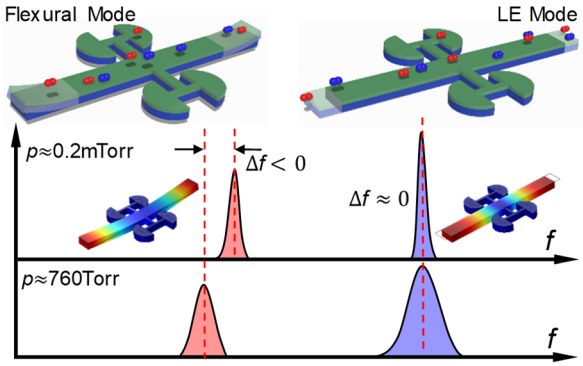

Figure 1: AlN/Si resonator vibrating at LE and flexural modes interacts with air molecules. The linewidths of both modes are broadened under atmospheric pressure. The frequency of flexural mode goes down while the frequency of bulk mode stays constant with increasing pressure level.

Another important factor in Eq. (1) is the medium loss. When the device is vibrating in moderate vacuum or near atmospheric pressure, the medium (air) damping can be an important dissipation mechanism which is heavily dependent on ambient pressure [7]. To date, many studies of pressure dependence and air damping have been conducted on traditional MEMS including cantilevers [7,8], doubly-clamped beams [9], and drumhead membrane resonators [10]. However, experimental investigation and analysis of pressure dependency of AlN/Si resonators is still lacking, especially for multiple modes. Moreover, a quantitative understanding of air damping effects in wider pressure range is of critical importance in designing and prototyping new MEMS technologies.

In this work, we present measurements and analyses of air damping effects on different modes of non-contact

electrically driven MEMS resonators fabricated in different heterostructure stacks. We carefully measure Q and f values for both length extensional (LE) mode and flexural mode (Fig. 1), as functions of ambient pressure from relatively high vacuum (10^{-4} Torr) to atmospheric level (760Torr) at room temperature. We find different modes of same device exhibit various tolerance to the air damping effects and provide quantitative evidences that could be helpful for future device engineering.

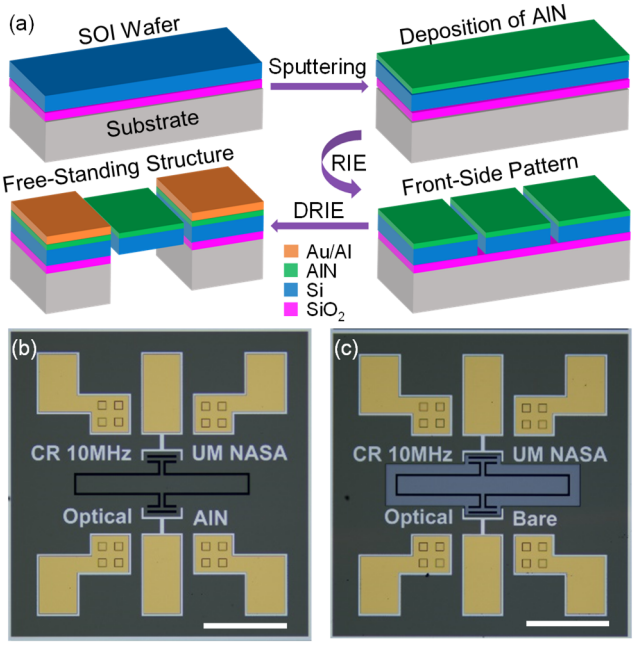

Figure 2: (a) Illustration of the AlN/Si device fabrication process using standard microfabrication techniques. RIE: reactive ion etching, DRIE: deep reactive ion etching. Optical images of (b) AlN/Si and (c) Si-only devices. Scale bar: 200μm.

FABRICATION AND EXPERIMENT

As illustrated in Fig. 2a, we begin the fabrication with a Si-on-insulator (SOI) wafer comprising a 20μm-thick n-type phosphorus (P) doped (at 4.6 ×10^{19} cm^{-3}) Si device layer and a 500μm-thick Si substrate. Next, on top of the highly doped Si layer, a 1μm-thick AlN layer is deposited to serve as the piezoelectric transducer. Then 100nm of aluminum (Al) is chosen for metal routing and patterned by lift-off process. We use photolithography to pattern the front side of the wafer followed by reactive ion etching (RIE) through the buried oxide (BOX) layer. To create suspended devices, deep reactive ion etching (DRIE) is performed from the back side of the wafer. Si-only devices are made by removing the top deposited AlN piezoelectric layer and metal electrodes. Figure 2b & 2c present the optical images of AlN/Si and Si-only BARs, respectively. The main body has a length of 415μm and a width of 43μm, and its center is attached to two tethers each of which is 35μm in length and 8μm in width.

Figure 3 presents the experimental scheme for the characterization of the resonant properties of the devices under varying pressure level. To efficiently excite the resonance motion of the device, we employ a non-contact overhanging electrode [6] connected to the output of a network analyzer (NA). The multimode resonances are simultaneously read out by focusing a 633nm red laser on the device employing ultrasensitive optical interferometry. The pressure is monitored via a pressure gauge connected to the chamber regulated by flow rate valves. We examine resonance behavior of the device from atmospheric pressure to high vacuum, then raise the pressure back to atmospheric conditions again. The measurements are carried out at room temperature.

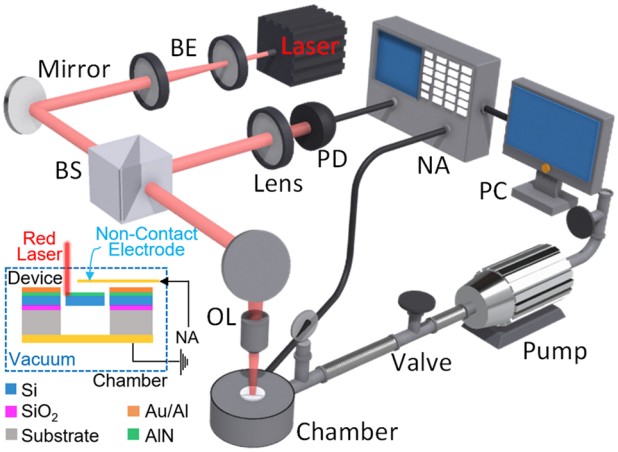

Figure 3: Schematic of measurement system using non-contact electric drive and optical detection. BE: beam expander, BS: beam splitter, NA: network analyzer, PD: photodetector, PC: personal computer, OL: objective lens.

RESULTS AND DISCUSSIONS

We first drive the LE bulk mode of the AlN/Si BAR and the resonance characteristics are clearly shown in Fig. 4a to 4f. To examine the pressure dependence of the damping, we measure and extract the f and Q at different pressure levels. Measured values of both parameters well overlap between sweeping-up and sweeping-down traces. As shown in Fig. 4a, the scheme resolves this mode at f=10.291MHz which roughly remains constant during the experiment. This may be a consequence of inappreciable influence from mass loading due to a large spring constant of LE mode and indicates a high immunity of LE mode to external pressure in terms of f stability. Moreover, we observe a p-independent Q when p is below 10Torr as the largest Q difference between Fig. 4d & 4f is less than 7%. This indicates that air damping impact is negligible in comparison to the intrinsic damping of the device itself. The independence of both f and Q on pressure within this pressure range suggests that dissipation is limited by other mechanisms (not air damping) for LE mode in p <10Torr region. Beyond 10Torr, Q declines with p and the measured tendency is consistent with the free molecule flow (FMF) damping which describes collisions of free air molecules with moving surface of the vibrating device. To examine if FMF is the primary dissipation mechanism, we have:

$$\left(\frac{1}{Q}\right)_{\text{tot}} = \left(\frac{1}{Q}\right)_{p\text{-indep}} + \alpha\left(\frac{1}{Q}\right)_{p\text{-dep}}, \qquad (2)$$

where $Q^{-1}_{p\text{-indep}}$ ($Q^{-1}_{p\text{-dep}}$) is the pressure independent (dependent) dissipation and α is a fitting parameter associated with device structure. The pressure dependent Q [10,11] is given by:

$$Q_{p\text{-dep}} = \frac{\rho t \omega_0}{4}\left(\frac{\pi RT}{2m}\right)^{\frac{1}{2}}\frac{1}{p}, \qquad (3)$$

where ρ is mass density of the device material, t is device

thickness, R is the gas constant, T is temperature, ω_0 is the resonance frequency of the selected mode, and m is the mass of gas molecule. Equation (2) is valid when the FMF becomes predominant pressure dependent dissipation process. Using this relationship, we find good agreement between fitting (red dashed curve) and measurement as depicted in Fig. 4a, and we determine α=0.58 through fitting to Eq. (2). This confirms that the air damping starts dominating the dissipation when p is above 10Torr for the LE bulk mode of AlN/Si device.

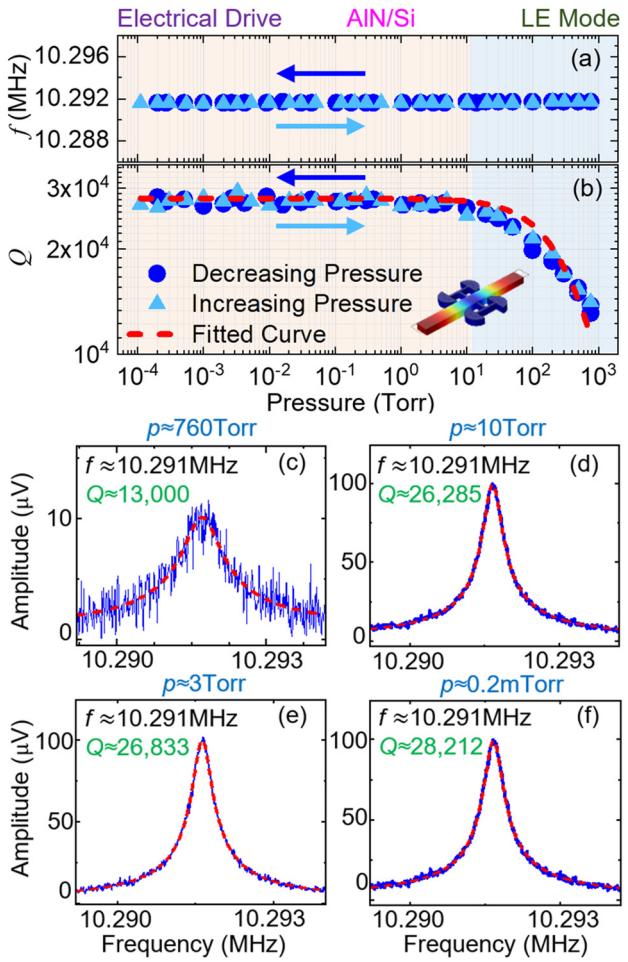

Figure 4: Measured resonance characteristics for the LE bulk mode of the AlN/Si resonator. (a)-(b): f and Q versus pressure. Red dashed curve shows the fitting to Eq. (2) with α=0.58. (c)-(f) Measured resonances with fitted Q values at p=760Torr, 10Torr, 3Torr, and 0.2mTorr.

We then excite the out-of-plane flexural mode of the AlN/Si device using non-contact electrical drive. As shown in Fig. 5, from 100μTorr to 1Torr, no clear influence from p on both f and Q is observed. The Q value extracted at 1Torr is only 0.8% lower than that extracted at 0.2mTorr. However, different from a stable f observed in the LE mode, the f of the flexural mode decreases as pressure goes to p> 1Torr. This may arise from the fact that the extent of mass loading has more apparent impact on flexural mode f due to its comparatively much smaller spring constant ($k_{\text{eff, flex}}/k_{\text{eff, LE}}$ ≈0.002). We apply Eqs. (2) and (3) to the measured trend of Q and the results agree well with fitting, which implies the air damping plays a role when p is above 1Torr for the flexural mode.

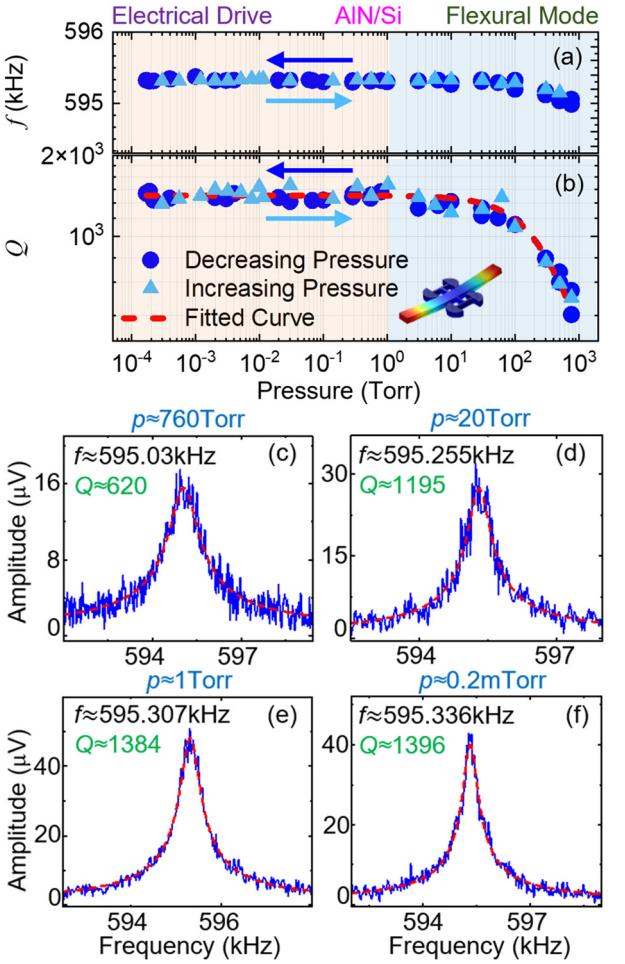

Figure 5: Measured resonance characteristics for the flexural mode of the AlN/Si device. (a)-(b): f and Q versus pressure. Red dashed curve shows the fitting to Eq. (2) with α=0.9. (c)-(f) Measured resonances at p=760Torr, 20Torr, 1Torr, and 0.2mTorr.

The Si-only device eliminates energy loss induced by loading and interfacial dissipation from the deposited metal electrode atop. Given its noticeably higher Q in the bulk mode [5,6] in comparison to that of the AlN/Si device, we also characterize the pressure dependence of its Q and f. As seen in Fig. 6, the LE bulk mode of Si-only device keeps a stable f of 10.127MHz with variations less than 0.001% throughout the measured pressure range. This LE mode maintains a high Q ≈ 257,000 with variation of 3% from the range p = 100μTorr to 3Torr. As the Q starts declining at p> 3Torr, the FMF model fits the data well with α = 0.79. Table 1 summarizes f and Q values for different modes in both devices at selected pressure levels.

CONCLUSION

In summary, air damping effects on both LE bulk and flexural modes of AlN/Si BAR, as well as LE mode of Si-only resonators, have been measured and analyzed. Using the non-contact electric drive for resonance excitation and a custom-built pressure-controlled apparatus, we have calibrated f and Q with p regulated from 760Torr to 100μTorr. We observe distinct features in the pressure-dependent resonance characteristics of dual modes: f of the LE bulk mode of AlN/Si resonator stays virtually constant

Table 1: Q factors and frequencies of the dual modes (LE & flexural) measured at various pressure levels.

Stacking \ Mode		Length Extensional (LE) Mode				Out-of-Plane Flexural Mode			
		760Torr	10Torr	3Torr	0.2mTorr	760Torr	20Torr	1Torr	0.2mTorr
AlN/Si	f (MHz)	10.291	10.291	10.291	10.291	0.59503	0.595255	0.595307	0.595336
	Q	13,000	26,285	26,443	28,212	620	1195	1384	1396
Si-Only	f (MHz)	10.127	10.127	10.127	10.127	No Data Taken			0.59474
	Q	20,213	124,357	227,500	235,600				961

over the entire pressure range while Q begins to degrade above 10Torr; the flexural mode of AlN/Si device exhibits stable f ≈595.3kHz below 1Torr but it falls to ≈595kHz at atmospheric pressure. The LE bulk mode of Si-only device shows stable f ≈10.127MHz independence of p, while it offers high Q ≈257,000 at p<3Torr. This work provides insight into distinct regimes in which air damping impacts the bulk and flexural modes of AlN/Si resonators, enhancing quantitative understanding that is beneficial for future device engineering and applications.

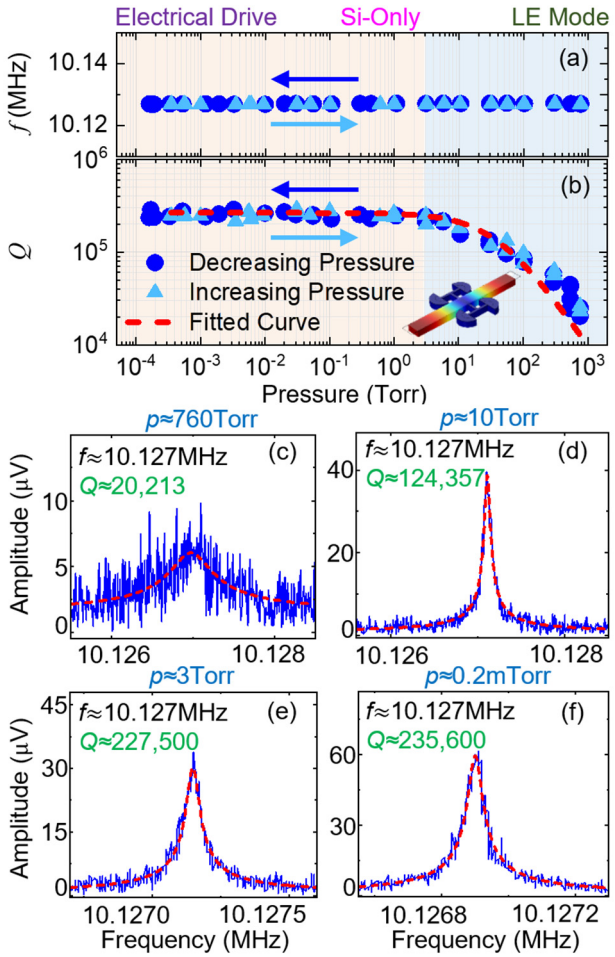

Figure 6: Measured resonance characteristics of the LE bulk mode of the Si-only resonator. (a)-(b): f and Q versus pressure. Red dashed curve shows the fitting to Eq. (2) with α=0.79. (c)-(f) Measured resonances at p=760Torr, 10Torr, 3Torr, and 0.2mTorr.

ACKNOWLEDGEMENTS

The effort at University of Florida (UF) is partly supported by National Science Foundation (NSF) CCF FET Program (Grant 2103091) and by the Margaret A. Ross Scholarship (S M Enamul Hoque Yousuf) in ECE at UF. The authors at UF thank X.-Q. Zheng and J. Lee for technical support and discussions.

REFERENCES

[1] R. Abdolvand, *et al.*, "Thin-Film Piezoelectric-on-Silicon Resonators for High-Frequency Reference Oscillator Applications", *IEEE Trans. Ultrason. Ferroelectr. Freq. Control*, vol. 55, pp. 2596-2606, 2008.

[2] J. L. Fu, *et al.*, "Dual-Mode AlN-on-Silicon Micromechanical Resonators for Temperature Sensing", *IEEE Trans. Electron Devices*, vol. 61, pp. 591-597, 2014.

[3] C. Fei, *et al.*, "AlN Piezoelectric Thin Films for Energy Harvesting and Acoustic Devices", *Nano Energy*, vol. 51, pp. 146-161, 2018.

[4] G. K. Ho, *et al.*, "Piezoelectric-on-Silicon Lateral Bulk Acoustic Wave Micromechanical Resonators", *J. Microelectromech. Syst.*, vol. 17, pp. 512-520, 2008.

[5] A. Qamar, *et al.*, "Study of Energy Loss Mechanisms in AlN-Based Piezoelectric Length Extensional-Mode Resonators", *J. Microelectromech. Syst.*, vol. 28, pp. 619-627, 2019.

[6] S M E. H. Yousuf, *et al.*, "Retaining High *Q* Factors in Electrode-Less AlN-on-Si Bulk Mode Resonators with Non-Contact Electrical Drive", *Proc. of the 35th IEEE Int. Conf. Micro Electro Mech. Syst. (MEMS 2022)*, pp. 979-982, 2022.

[7] J. Yang, *et al.*, "Energy Dissipation in Submicrometer Thick Single-Crystal Silicon Cantilevers", *J. Microelectromech. Syst.*, vol. 11, pp. 775-783, 2002.

[8] J. E. Sader, *et al.*, "Frequency Response of Cantilever Beams Immersed in Viscous Fluids with Applications to the Atomic Force Microscope", *J. Appl. Phys.*, vol. 84, pp. 64-76, 1998.

[9] S. S. Verbridge, *et al.*, "A Megahertz Nanomechanical Resonator with Room Temperature Quality Factor Over a Million", *Appl. Phys. Lett.*, vol. 92, art. no. 013112, 2012.

[10] J. Lee, *et al.*, "Air Damping of Atomically Thin MoS_2 Nanomechanical Resonators", *Appl. Phys. Lett.*, vol. 105, art. no. 023104, 2014.

[11] W. E. Newell, *et al.*, "Miniaturization of Tuning Forks: Integrated Electronic Circuits Provide the Incentive and the Means for Orders-of-Magnitude Reduction in Size", *Science*, vol. 161, pp. 1320-1326, 1968.

CONTACT

†*Equally Contributed Authors*

*†Yuncong Liu: yuncong.liu@ufl.edu

*†S M Enamul Hoque Yousuf: syousuf@ufl.edu

* Mina Rais-Zadeh: mina.rais-zadeh@jpl.nasa.gov

* Philip Feng: philip.feng@ufl.edu